Prins cyclization of (-)-isopulegol with benzaldehyde for production of chromenols over organosulfonic clays

Li-Zhulanov, Nikolai; Mäki-Arvela, Päivi; Laluc, Mathias; Peixoto, Andreia F.; Kholkina, Ekaterina; Sandberg, Thomas; Aho, Atte; Volcho, Konstantin; Salakhutdinov, Nariman; Freire, Cristina; Sidorenko, Alexander Yu.; Murzin, Dmitry

Published in:
Molecular Catalysis

DOI:
10.1016/j.mcat.2019.110569

Published: 01/01/2019

Document Version
Accepted author manuscript

Document License
CC BY-NC-ND

Prins cyclization of (-)-isopulegol with benzaldehyde for production of chromenols over organosulfonic clays

Nikolai Li-Zhulanov[a,c,d], Päivi Mäki-Arvela[a], Mathias Laluc[a], Andreia F. Peixoto[b], Ekaterina Kholkina[a], Thomas Sandberg[a], Atte Aho[a], Konstantin Volcho[c,d], Nariman Salakhutdinov[c,d], Cristina Freire[b], Alexander Yu. Sidorenko[e], Dmitry Yu. Murzin[a,*]

[a] *Åbo Akademi University, 20500 Turku/Åbo, Finland*

[b] *LAQV-REQUIMTE, Departamento de Química e Bioquímica, Faculdade de Ciências, Universidade do Porto, Rua do Campo Alegre s/n, 4169-007 Porto, Portugal*

[c] *Novosibirsk Institute of Organic Chemistry, Lavrentjev av. 9, 630090, Novosibirsk, Russian Federation,*

[d] *Novosibirsk State University, Pirogova st. 1, 630090, Novosibirsk, Russian Federation,*

[e] *Institute of Chemistry of New Materials of National Academy of Sciences of Belarus, 220142, Skaryna str. 36, Minsk, Belarus*

**Corresponding author: dmurzin@abo.fi*

ABSTRACT

Prins cyclization of (-)-isopulegol with benzaldehyde was investigated with sulfur containing halloysite nanotubes, K10 clays and Cloisite clays. The catalysts were characterized by TEM, SEM, XRD, XPS, pyridine adsorption desorption by FTIR, nitrogen adsorption. The most active catalyst was K10 modified with chlorosulphonic acid giving 95 % selectivity to the desired chromenol at 90 % conversion and 30 ^{o}C. Selectivity to chromenol was increasing with increasing Lewis acid site concentration while no linear correlation of chromenol selectivity with the Brønsted acid sites concentration was observed. The diastereoisomer *R/S* ratio of chromenols was the highest, 11.5, at 70 °C and 90 % conversion over sulfur modified halloysite nanotubes exhibiting rather low acidity. A higher stability of the *R*-isomer confirmed by quantum mechanical calculations can partially explain preferential formation of the *R* diastereomer.

Successful catalyst reuse was demonstrated with the best performing catalyst, organosilylated sulfur containing K10.

Key-words: Organosulfonic clays; Prins reaction; chromenols; isopulegol

1. Introduction

Naturally occurring, cheap and abundant compounds are important raw materials for value added chemicals, such as pharmaceuticals and fragrances. One interesting group of drugs are compounds with a benzopyran scaffold, chromene, which exhibit biological activity [1]. (-)-Isopulegol has been used as a starting reagent for synthesis of chromenols [2-5]. This intermediate is prepared from naturally occurring citronellal present in citronella oil. Cyclization of citronellal is a well-established route, which has been extensively studied over homogeneous and heterogeneous acid catalysts [6,7]. Production of chromenol proceeds via condensation of (-)-isopulegol with aldehydes, as shown in Scheme 1. In this reaction two different diastereoisomers, *4R* and *4*S, are formed in addition to the undesired dehydration product. It has been reported that especially high analgesic activity was demonstrated for 4R diastereoisomer of the chromenol containing sulfur [8]. This product was synthesized starting from isopulegol with thiophene-2-carbaldehyde.

Several aromatic aldehydes including vanillin [10], benzaldehyde [2,3, 4] as well as halogenated and nitrated aldehydes [11] and aliphatic ones, e.g. citronellal e.g. citronellal [5, 6] have been used as starting reagents for production of chromenol including halogenated and nitrated aldehydes. Chromenol has been synthesized over homogeneous [12] and heterogeneous catalysts [2,3, 4, 13]. One inexpensive heterogeneous catalyst is K10 clay, over which chromenol was synthesized in the absence of any solvent, however, enhancing the reaction with microwave irradiation for 3 min at room temperature giving 76 % yield of chromenol with the R/S ratio of 9/1 [14]. Since the product has a rather large size, 0.7 – 0.9 nm [3], also mesoporous Ce-modified silicate material, MCM-41 [2] and micro-mesoporous ZSM-5 derived catalysts were successfully applied in the synthesis of chromenols [3]. Recently montmorillonite clays K10, K30 and HCl treated

halloysite nanotubes were used as catalysts for synthesis of various chromenols [4]. The highest selectivity to phenyl-substituted chromenol (79 %, sum of B+C in Scheme 1) was observed over halloysite at 20 ^{o}C in cyclohexane. Moreover, a very high 4R/4S ratio of 14.5 was achieved which was associated with the presence of weak Brønsted acidity in nanotubes [4]. Further experimental work and kinetic modelling allowed to suggest a dual mechanism of catalyst action involving formation of an intermediate with the subsequent transfer of water from nanotubes surface to the intermediate, which led to selective formation of the *R*-isomer [15].

In this work the performance of organosulfonic acid modified halloysite nanotubes (HNT), montmorillonite K10 (K10) and cloisite-Na^+ (CLOI) clays as acid catalysts in Prins cyclisation of (-)-isopulegol was evaluated and compared. Organosulfonation of has been applied to modify various supports, such as SBA-15, to prepare sulfonated silica catalysts, which have been successfully used in condensation of acetone and aniline [16]. In the current work the organosulfonic acid grafting of clays was performed using two different modification methodologies, namely direct sulfonation with chlorosulphonic acid and one-pot organosilylation with 2-(4-chlorosulfonylphenyl)ethyltrimethoxysilane (Scheme 2) as reported in [17, 18]. Halloysite is a cheap naturally occurring mineral material [19] with unique physicochemical properties and potentially a wide application range including catalysis. HSO_3-functionalized HNT were successfully used, for example, in esterification of free fatty acids for production of biodiesel [17]. Cloisite Na^+ is a natural montmorillonite commercially used as a filler in polymer industry [20]. K10 is already used as intrinsic catalyst including in the synthesis of chromenols [4]. However, organosulfonic acid functionalization of these clays based montmorillonites are not yet well explored [21,22]. Recently, several organosulfonic acid functionalized K10 and

Cloisite Na^+ were successfully prepared and used as solid catalysts for (trans) esterification of free fatty acids and (waste) oils [23].

2. Experimental

2.1.Reagents and equipment

Montmorillonite K10, Halloysite nanotubes, anhydrous toluene (99.8 %), were purchased from Sigma Aldrich, chlorosulfonic acid (≥ 98 %) from Fluka; 2-(4-chlorosulphonylphenyl)ethyltrimetoxysilane (CSPTMS, 50 % in methylene chloride) from ABCR GmbH; Cloisite-Na^+ was kindly provided by Southern Clay. Unless stated otherwise, all reagents were used without further purification. (-)-isopulegol (Sigma Aldrich, ≥ 98%) and benzaldehyde (Sigma Aldrich, ≥ 99 %) were used without further treatment. Argon gas was purchased from AGA (99.999 %).

2.2 Catalysts preparation

2.2.1 Synthesis of HNT_CSP, CLOI_CSP and K10_CSP catalysts

The catalysts were prepared according to reported methodologies [17, 23] as follows**:** 2.0 g of material was dispersed in 100 ml of anhydrous toluene or CH_2Cl_2; this suspension was kept under vigorous stirring for 5 min. Subsequently, addition of 2-(4-chlorosulfonylphenyl)ethyltrimethoxysilane (CSP) (1.84 ml, 7.8 mmol) was carried out and the reaction was maintained at 120 °C under magnetic stirring and an inert atmosphere for 24 h. After this period, the functionalized CSP materials were recovered by filtration or centrifugation, washed under 100 ml of toluene and/or CH_2Cl_2 under reflux, filtrated and finally dried at 100 ° C for 24 h.

2.2.2 Synthesis of HNT_CSA, CLOI_CSA and K10_CSA catalysts

These catalysts were prepared by direct sulfonation of CLOI and K10 with chlorosulphonic acid (CSA) according to the literature [23]: 2.0 g of clay and 35 ml of dichloromethane were transferred to a flask and the suspension was kept under magnetic stirring in an ice bath for 10 min during which 2 ml of $ClSO_3H$ was added dropwise through a funnel. Thereafter, the solution was stirred at room temperature for 4 h. Finally, the functionalized CSA materials were filtered, washed with methanol and dried at 100 °C for 24 h.

2.3. Catalyst characterization methods

Elemental analysis (EA) – C, H and S – was obtained with a LECO equipment (CHNS-932 model) using a sample size between 0.01-2.0 mg with a precision and reproducibility lower than 0.03 and 0.2 %, respectively.

X-ray photoelectron spectroscopy (XPS) was performed using a Kratos AXIS Ultra HSA, coupled with VISION software for data acquisition, at Centro de Materiais da Universidade do Porto (CEMUP), Porto, Portugal. The equipment used a monochromatic Al Kα X-ray source (1486.7 eV); operation conditions: 15 kV (90 W); Fixed Analyser Transmission (FAT) mode; 40 eV (regions ROI) and 80 eV (survey) of pass energy. Samples in the powder form were pelletized under pressure before XPS analysis. Data acquisition was performed with a charge neutralization system under vacuum ($<1\times10^{-6}$ Pa). C1s band at 285.0 eV was used as an internal standard for binding energy (BE) calibration. CASAXPS software was selected for data analysis.

The acid capacity of the catalysts, in mmol H^+/g, was obtained by potentiometric titration, using HACH TitraLab AT 1000 (electrode assembly PHC705 by HACH). 0.5 g of a solid catalyst was suspended in 50 ml of 2 M NaCl. The suspension was maintained

at room temperature and under stirring for 24 h. Finally, the mixture was filtered and the final solution was titrated with 0.025 M NaOH [24].

Pyridine adsorption desorption was investigated using FTIR ATI Mattson instrument in the following way: the catalyst was pretreated at 100 ºC for 1 h, thereafter pyridine was adsorbed at 100 ºC for 30 min. Pyridine desorption was recorded at 100 ºC after 15 min desorption. Determination of acid strength distribution with pyridine as a probe molecule is typically done by desorbing it at different temperature between 250 ºC and 450 ºC. In the current case such determination was not done as the thermal stability of the modified clays is limited to 140 ºC. The quantification of Brønsted and Lewis acid sites was made using the extinction factor of Emeis [25].

Powder X-ray diffraction (XRD) measurements were performed at room temperature with a Siemens D5000 diffractometer using Cu Kα radiation (λ = 1.5406 Å) and Bragg–Brentano $\theta/2\theta$ configuration.

The N_2 adsorption isotherms were determined at −196 ºC in a Quantachrome NOVA 4200e multistation apparatus, LSRE-LCM, Departamento de Engenharia Química, Faculdade de Engenharia do Porto, Portugal. Samples were previously degassed at 150 ºC for 3 h.

The SEM/EDS was performed using a High resolution (Schottky) Environmental Scanning Electron Microscope with X-Ray Microanalysis and Electron Backscattered Diffraction analysis: Quanta 400 FEG ESEM / EDAX Genesis X4M, Centro de Materiais da Universidade do Porto, Portugal. The samples were prepared and analyzed directly as powders, uncoated and coated with a Au/Pd thin film, for 100 sec. and with a 15mA current, by sputtering, using the SPI Module Sputter Coater equipment. Some measurements were also performed with LEO Gemini 1530 with a Thermo Scientific UltraDry Silicon Drift Detector equipped with a secondary electron, a backscattered

electron and an In-Lens detectors. Determination of the elemental composition was done using Energy dispersive X-ray micro-analysis spectroscopy (EDX).

The nanoscale structure of the catalysts were investigated with transmission electron microscopy using a JEM 1400 plus instrument with an acceleration voltage of 120 kV and a resolution of 0.98 nm utilizing a Quemsa II MPix bottom mounted digital camera.

The Fourier transform infrared spectroscopy-attenuated total reflectance (FTIR-ATR) spectra were obtained on a Perkin-Elmer Spectrum 100 Series spectrophotometer equipped with an ATR accessory (diamond/ZnSe) in the range of 650–4000 cm^{-1}.

The thermogravimetric analysis (TG) was performed in a Pyris 1 TGA, PerkinElmer using 10–15 mg of the samples heated under air flow (20 cm^3/min) to 900 °C at a rate of 10 °C/min.

2.4 Experimental setup and analysis

In a typical experiment isopulegol with an initial concentration of 0.013 mol/l in benzaldehyde was loaded into the reactor containing 0.1 g of the dried catalyst. The reaction was performed under in flowing argon in a glass reactor equipped with a reflux cooler either at 30 or 70 ^oC using small catalyst particles (below 90 µm) under intensive stirring (390 rpm) to avoid both internal and external mass transfer limitations.

The samples were analyzed by a gas chromatograph equipped with HP-5 column (length 30 m, diameter 0.32 mm, film thickness 0.5 µm) using the following temperature programme: 100 ^oC (5 min) – 10 ^oC/min- 280 ^oC (10 min). The unidentified products were confirmed by GC-MS.

2.5. Quantum Mechanical Calculations/Computational methods

In order to evaluate if different behavior of the *R* and *S* diastereomers of chromenol due to the intrinsic differences of the two molecules, ESP-fitting charges, bond orders and protonation energies were evaluated computationally.

The stability of *R*- and *S*-chromenols was studied by a multi-level deterministic structural optimization using the *Forcite, Conformers* and *DMol3* modules in the software *Materials studio 2019* version 19.1.0 [26, 27]. At molecular mechanics (MM) level, the Universal Force Field was applied as implemented in the *Conformers* module. The most stable conformers were optimized with density functional theory applying the B3LYP hybrid functional [28-31], the TNP (*triple-zeta*) basis set and Grimme's method for DFT-D (dispersion) correction [32] as implemented in the *DMol3* module. Vibrational frequencies were also calculated in order to obtain thermodynamic data of the stabilities.

The surrounding medium might determine which conformation will be preferred. In order to corroborate this, the systems were studied in solutions applying the COnductorlike Screening MOdel (COSMO) [33] with the dielectric constant 20.7 for acetone.

3. Results and Discussion

3.1. Characterization of the catalysts

XRD patterns of different catalysts are shown in Fig. 1. For cloisite Na^+ the d_{001} spacing was determined to be 1.2 nm (Table 1), which is in line with [34]. The XRD for HNT catalysts were already reported in [17] showing the reflection plane (001) at 11.97° and no significant structural variations of modification were observed. When modification with CSA or CSP was made, a slight increase of d_{001} was observed indicating an expansion of clay mineral interlayer. This interlamellar expansion for HNT was not visible for HNT and K10 clays after modification.

SEM image of HNT _CSP (Fig. 2a) showed that presence of 100-600 nm tubes confirmed as well by TEM. SEM-EDXA results revealed that Si/Al weight ratio for halloysite clay was 1.18 while the theoretical ratio is 1.04 calculated from its clay with the molecular formula of $Al_2Si_2O_5(OH)_4.2H_2O$ [35]. The increased ratio is due to organosilylation of the parent material. TEM results showed that HNT_CSP exhibited nanotubes with the diameter of 31 nm and the wall thickness of 14 nm. The length of these tubes varies in the range 100 – 600 nm (Fig. 2b,c), while the diameter is 90 nm, similar to [36].

SEM images of CLOI_CSP (Fig. 2d) showed in addition to the conventional shape of cloisite, i.e. irregular thin flakes, also round shaped large SiO_2 particles with the size of ca. 1 μm**.** The Si/Al ratio of CLOI_CSP was calculated based on its elementary composition, $Na_{0.75}(Al_{3.25}Mg_{0.75})(Si_8O_{20})(OH_4)$ [37] being 2.56. The measured weight ratio of Si/Al was 3.0 showing again the presence of silicon originating from organosilylation. In the TEM image of CLOI_CSP 400 nm long parallel oriented fibres which 1.3 nm broad interlamellar space are visible (Fig. 2e,f). It can be seen from Fig. 2 e that CLOI_CSP contained also large ball shaped particles with the size up to 420 nm, which can be most probably attributed to silica as Si/Al ratio in CLOI_CSP was enriched.

The SEM image of K10_CSP (Fig. 2g) showed presence of irregular shaped layered particles analogously to [37]. EDXA analysis of this material resulted in the Si/Al weight ratio of 5.4, while in [13] it was lower, i.e. 4.8, which is due to organosilylation of K10_CSP. In the TEM image of K10_CSP both fibres and crystals are visible (Fig. 2h,i). The fibres of ca. 10 - 40 nm long were in parallel bundles with a rather small interlamellar distance of 1-2 nm which is in accordance with XRD.

The elemental analysis of different catalysts shows (Table 2) that nearly the same sulphur content was obtained with HNT modification using CSA and CSP as modifiers.

On the other hand, more sulphur was attached to K10 from CSA than from CSP and the opposite is valid for CLOI modification. The total sulphur concentration was, however, lower than the surface sulphur content determined by XPS for HNT and K10_CSA as already discussed above. An increased Si/Al ratio is observed for HNT_CSP due to its silylation [17]. XPS results showed that the sulphur content on the catalyst surface decreased in the following order: K10_CSA > HNT_CSP > HNT_CSA > CLOI_CSA > CLOI_CSP > K10_CSP (Table 3). It can also be seen that surface enrichment of sulphur occurred for HNT and K10_CSA since the amount of sulphur recorded by XPS was higher than determined by the elemental analysis. These results are in line with XRD results for HNT and K10_CSA, which did not show any interlamellar expansion of the clay. The S content of HNT_CSP (Table 3) on the surface is rather high suggesting that the sulfonic acid groups are preferable covalently linked on the outer HNTs surface defects and on the edges.

For K10 catalysts the Si/Al ratio was higher than for the parent material due to silylation. On the other hand, a lower Si/Al ratio in comparison to the parent K10 was observed for K10_CSA due to the presence of sulphur on the catalyst surface. For K10 catalysts the carbon content for K10_CSP was also increased, as expected due to the presence of phenyl group, in comparison to the parent material (Table 3). In case of CLOI catalysts (Table 3) the Si/Al ratio for CLOI and CLOI-CSA was about the same, while CLOI-CSP it was increased by 10 % in comparison to the parent material. The carbon content of CLOI_CPS was also 1.8 fold that of the parent material due to presence of the phenyl group (Table 3).

The specific surface areas and pore sizes were determined by nitrogen adsorption-desorption showing that after functionalization of K10 the specific surface area decreased with a significant impact on K10_CSA, being only 16 % of the pristine material (Table

2). The specific surface area reported for K10 is in line with the one reported in the literature being 241 m^2/g_{cat} [38]. A very low specific surface area was recorded for CLOI_CSP in comparison to CLOI_CSA indicating pore blockage for the former one. The specific surface areas of modified HNT catalysts were also low in accordance with the low value reported in literature for the pristine HNT, 65 m^2/g_{cat} [39].

Acidity of the catalysts was determined both with potentiometric titration and pyridine FTIR (Table 4). The results showed the most acidic catalyst was K10_CSA followed by HNT_CSA and in all cases CSA modified catalysts were more acidic than CSP modified ones. According to pyridine-FTIR CSA modified catalysts exhibited a higher concentration of Brønsted acid sites in all other series except CLOI_CSP containing more Brønsted acid sites than CLOI_CSA (Table 4). The amount of Lewis acid sites was higher for all other CSA modified catalysts except for K10_CSA, which contained no Lewis acid sites.

The results from FTIR-ATR (Fig. 3) show differences in the pristine and modified catalysts. HNT exhibits the typical bands at 3691 and 3624 cm^{-1} corresponding to the stretching vibrations of the structural hydroxyl groups [40] and the presence of adsorbed water with a band at 1643 cm^{-1} [17]. The vibrational band at 1001 cm^{-1} is characteristic for Si-O stretching vibrations [17]. The bands at 3633 cm^{-1}, 1048 cm^{-1} in CLOI and K10 correspond also to O-H and Si-O-Si, respectively [41] similarly to the band at 1643 cm^{-1} for water [17]. For K10 the characteristic peak at *ca.* 795 cm^{-1} corresponding to quartz as an impurity is clearly visible [42] together with the above-mentioned water, OH and Si-O-Si bands. Overall it can be stated that the structures were retained after sulphur modification.

The TGA results (Fig. 4) indicate that weight loss in the temperature range of 100 – 900 ^oC decreased as follows: HNT_CSP > CLOI_CSP > K10_CSP > HNT_CSA >

K10_CSA = HNT_CSA >> CLOI_CSA. The weight losses for K10, HNT and CLOI modified with CSP are higher in the range of 400-600 ºC and are attributed to decomposition of the organic chain of the organosilanes covalently linked and/or dehydroxylation.

3.2 Catalytic Results

3.2.1. Initial rates and conversion

Six different modified clays were investigated in Prins cyclization of (-)-isopulegol at 70 ºC (Table 5, Fig. 5a). The results revealed that the highest initial rates at 70 ºC were obtained with K10_CSA with high Brønsted acid site concentration. The lowest rates are recorded for HNT modified catalysts, which exhibited the lowest concentration of Brønsted acid sites among all the studied catalysts. Especially the reaction rates with HNT catalysts declined after 15 min reaction time 8 fold in comparison to the initial rate (Fig. 5a). It is also interesting to note that the most active catalyst K10_CSA exhibited no Lewis acid sites, Table 4. It can thus be concluded that the reaction rate is proportional to the concentration of Brønsted acid sites.

The effect of temperature was also investigated for the two most active catalysts, K10 and CLOI modified catalysts (Table 5). The parent K10 was also investigated giving a lower initial rate and longer time to reach complete conversion in comparison to K10-CSA and K10-CSP (Table 5). Functionalized catalysts exhibit higher acidity compared to the parent K10 explaining a higher rate in the former case. K10 catalyst in the current study gave a higher conversion than the one obtained in [11] at 25 °C where it was concluded that an acid modified K10 catalyst was more efficient than the parent one.

The initial rate decreased at 30ºC in the following order: K10_CSP ≈ K10_CSA > CLOI-CSP. The Brønsted acid concentration (Table 4) did not exhibit a clear effect on the initial rate at low temperature, in opposite to the results at 70 ºC.

The conversion increased with increasing reaction time both at 30 ºC and 70 ºC for all catalysts showing that they were not fully deactivated (Fig. 5a, 6a) and it was possible to obtain almost complete conversion with all catalysts in 240 min (Table 5).

3.2.2. Product distribution

The selectivity to chromenols and product D in Prins cyclization of (-)-isopulegol with benzaldehyde are shown as a function of the concentration of Brønsted and Lewis acid sites in Figures 7a and 7b. Selectivity towards the desired product, the mixture of *R* and *S* chromenol, (Scheme 1) varies in the range of 35 – 95 % (Table 5). A low reaction temperature favored formation of chromenols suppressing further dehydration and the highest selectivity to this mixture was obtained at 30 ºC K10-CSP, being 95 % at 90 % conversion.

K10_CSP catalyst exhibited the highest amount of Lewis acid sites (Table 4). When selectivity to chromenol at 90 % conversion is plotted as a function of the concentration of Brønsted and Lewis acid sites (Fig. 6c), it can be seen that selectivity increased with increasing Lewis acid site concentration (Fig. 7b), while the selectivity trend with increasing Brønsted acid site concentration at 70ºC was not linear (Figure 7a). Note that in the presence of a strong Brønsted acid (Amberlyst-15 resin), formation of predominantly dehydration products was observed [15].

On the other hand, for HNT and CLOI modified catalysts selectivity increased with increasing Brønsted acid site concentration. The trend of selectivity to chromenol vs concentration of Lewis acid site concentration was declining at 70ºC for K10 and CLOI

modified catalysts, while HNT modified catalysts exhibited a similar trend as obtained at 30^{o}C, Fig. 7b. This result indicates that not only acidity, but also temperature is very important parameter affecting the selectivity to chromenols.

Selectivity to chromenols in Prins cyclisation of (-)-isopulegol with benzaldehyde at 70 ^{o}C increased with increasing Lewis acidity as mentioned above (Fig. 7b). There is no linear correlation between selectivity to chromenols and the amount of Brønsted acid sites (Fig. 7a). Moreover, even an optimum amount of Brønsted acid sites could be suggested for the maximum in selectivity. As a comparison with literature [4], 79% selectivity to chromenols was reported at 20^{o}C over a modified halloysite at 50 % conversion. It should, however, be pointed out that a higher selectivity to chromenol was obtained at a lower temperature. In the current work it was observed that a lower temperature gave higher selectivity to chromenols for both K10 and CLOI modified catalysts (Table 5). The highest selectivity was obtained with K10-CSP.

The *R/S* ratio is also an important parameter determining the product properties. The *R/S* ratio declined in the following order: HNT_CSP > CLOI_CSP > K10_CSP > K10_CSA > HNT_CSA > CLOI_CSA at 70^{o}C and this ratio was nearly constant with increasing conversion (Fig. 5b). A slightly higher *R/S* ratio was obtained for K10_CSP and CLOI_CSP modified clays at 30^{o}C (Table 5). The *R/S* ratio was higher for mild Brønsted and Lewis acidic catalysts and higher for CSP modified catalysts than CSA modified ones (Fig. 8). In the current work the highest *R/S* ratio (11.5) was obtained over HNT_CSP at 70^{o}C. In the work of Sidorenko et al. [4] the highest *R/S* ratio, 14.5 was obtained at 20^{o}C using pristine HNT as a catalyst. This result is not directly comparative with the current results due to a lower reaction temperature in [4], which might increase R/S ratio as discussed above. Furthermore, when using the functionalized HNT_CSP, the physically adsorbed water exhibiting weak Brønsted acid sites on the HNTs surface was

substituted during organosilylation [39] by stronger $–SO_3H$ groups, which might also decrease the *R/S* ratio. On the other hand, note that HNT has the lowest acidity (Table 4). According to [13, 15], the isomers ratio increased with decreasing catalyst acidity.

In general, formation of tetrahydropyran compounds is suggested to occur through aliphatic alcohols with an allyl moiety. In the presence of both weak Lewis and Brønsted acids (for example, $ZnBr_2$ and HOAc), an intermediate cyclic carbocation is formed with a subsequent capture of the nucleophile from the catalyst (for example, Br^-) resulting in halide-substituted tetrahydropyran formation [43]. A synergistic effect between the Lewis and Brønsted acids was found, leading to an increase in the acidity of the latter [43].

Condensation of aliphatic phenyl-substituted alcohol with benzaldehyde in the presence of Lewis acids, especially $FeCl_3$, resulted in the stereoselective formation of tetrahydropyran-4-ols [44] and dehydration products, however, without giving other by-products such as hemiacetals. According to the theoretically predicted and experimentally confirmed mechanism, aldehyde oxygen and alcohol hydrogen participate in the formation of the hydroxyl group [44]. Rather selective (70%) formation of tetrahydropyran-4-ols was also observed in the presence of methyltrioxorhenium as a Lewis acid [45].

In a recent publication [15], stereoselective formation of 4*R*-isomer of chromenol in the presence of air-dry halloysite nanotubes was explained by the transfer of water from halloysite surface to the intermediate, giving predominantly the single stereoisomer. Note that water molecules on the surface of aluminosilicates can be coordinated by the Lewis acid sites and act as weak Brønsted acids ($H^{\delta+}\cdots OH^{\delta-}$), followed by transfer of $OH^{\delta-}$ as a nucleophile [15], which is similar to the synergistic effect described in [41]. Thus, the mechanism of water transfer from heterogeneous catalyst, first discussed in [1],

can be considered as a special case of a more general mechanism for formation of compounds with a tetrahydropyran moiety proposed in [43].

In the present work, a high overall selectivity to chromenols was observed in the presence of modified clay K10-CSP at 30 ºC, while there was a trend of increasing selectivity with increasing Lewis acidity (Fig. 6c). K10-CSP material was dried before the reaction, which eliminates a critical involvement of water in this reaction. Moreover, only formation of chromenols and dehydration products was observed. Thus, a high overall chromenol selectivity on K10-CSP can be explained by the reaction proceeding according to the mechanism similar to the one described in [44].

In the current work quantum chemical calculations were performed to fill the apparent gap in understanding of the product distribution. Three different structures are formed in the condensation of isopulegol with benzaldehyde, i.e. chromenol *R*- and *S*-diastereomers and the dehydrated product, D (Scheme 1) (Table 6) with *R*-diastereomer being the main product. This is in line with the quantum mechanical calculations showing that this product is more stable than the *S*-diastereomer by 5.4 kJ/mol at the DFT/B3LYP/TNP level (Fig. 9). The standard thermodynamic quantities in the temperature range of 275 – 375 K are given in Tables 6 and 7. At 300 K and 350 K respectively, the Gibb's free energy was 820.7 and 793.7 kJ/mol for the R-diastereomer and 816.5 and 790.0 kJ/mol for the S-diastereomer.

No clear differences between the diastereomers could be seen in the ESP-fitting charges or bond orders, showing the charge –0.73 for oxygen in the hydroxyl group and Mulliken C–O bond order 0.69 for *S* and 0.71 for *R*-chromenol. This result indicates that thermodynamics is not the primary origin for decreasing *R/S* ratio during the reaction associated with its further dehydration to product D. Thus the solid catalyst can have

steric constrains which facilitate further reaction of *R*. Similar suggestions about the steric constrains were proposed in [4] based on kinetic analysis.

The main side product in the Prins reaction is the dehydration product of *R*-chromenol (D in Scheme 1). According to a two-step mechanism discussed in [4], a cationic intermediate is generated by dehydration followed by hydroxylation giving both *R*- and *S*-chromenol. Thereafter, *R*-diastereomer is more prone to dehydration forming the dehydrated product D. This dehydration occurs on the strong acid sites. Plotting the concentrations of dehydration product and chromenol (Fig. 10) gives the ratio between the initial rates for formation of dehydration product and chromenol allowing to conclude that HNT_CSP catalyzed 3.1 fold more intensively formation of the dehydration product in comparison to CLOI_CSP. The lowest initial rates for formation of the dehydration product were obtained over K10_CSP (Fig. 9). HNT_CSP contains a large amount of *S* on the surface favoring formation of the dehydration product. On the other hand, K10_CSP and CLOI_CSP contain the sulfonic acid groups in the interlayers (this is also corroborated by XRD results) and consequently a more hindered accessibility of H^+ is expected.

3.2.3. Reproducility tests

The reproducibility test in Prins cyclization of (-)-isopulegol with benzaldehyde was performed over the best catalyst, K10_CSP, at 30ºC showing that conversion of (-)-isopulegol is nearly the same in two different experiments (Fig. 11a). Difference in the concentration of chromenols (Fig. 11b) is ascribed to the difference in the liquid phase mass balance.

3.2.3. Filtrate test and catalyst reuse

For the best performing catalyst, K10_CSP, a filtrate test was performed to investigate if some sulfur would be leached out (Fig. 12). The results showed that when the catalyst was filtrated between 20 – 60 min the reaction proceeded even without stirring. At 60 min a liquid sample was taken and the reaction with the filtrate was started. The results revealed that (-)-isopulegol was not further converted in the absence of the catalyst showing clearly that sulphur is not leached into the liquid phase and the only heterogeneously catalyzed reaction can occur.

For the best catalyst, K10_CSP, its reuse was investigated both by washing the once used catalyst either with toluene or dichloromethane. The results showed that declined rates were obtained giving the final conversion levels of 96% and 77% with these solvents, respectively after 240 min. The selectivity towards chromenols with the fresh and toluene washed reused K10-CSP catalyst at 90 % conversion levels were 95 % and 88 %, respectively, being also a rather promising result showing that toluene washing is preferential giving also a high conversion of (-)-isopulegol.

4. Conclusions

Prins cyclization of (-)-isopulegol with benzaldehyde was investigated with halloysite nanotubes, K10 and Cloisite Na^+ clays modified either with chlorosulphonic acid or grafted with chlorosulfonylphenyl-ethyltrimethoxysilane. The highest amount of sulphur was present in K10 modified with chlorosulphonic acid, while the lowest sulphur content was observed in halloysite nanotubes. X-ray photoelectron spectroscopy also revealed that Cloisite modified clays exhibited a relatively low amount of sulphur on the surface opposite to halloysite nanotubes.

The most active catalyst was K10 catalysts modified with chlorosulphonic acid, while the most selective one towards the desired chromenols was organosilylated sulphur containing K10 clay. The highest selectivity was obtained with this catalyst at 30 °C being 95 % at 90 % conversion. It was also observed that chromenol selectivity increased with increasing concentration of Lewis acid sites, while there was no linear correlation between selectivity to chromenol and the concentration of Bronsted acid sites. The diastereoisomer *R/S* ratio of chromenols was typically rather constant with increasing conversion. The highest *R/S* ratio, 11.5 at 90% conversion was obtained with halloysite nanotubes at 70°C. This catalyst exhibited also a slow rate. For several catalysts tested both at 30 °C and 70 °C the *R/S* ratio was higher at the lower reaction temperature. The origin for the higher formation of R-diastereomer was attributed to a higher stability of the R-isomer confirmed by quantum mechanical calculations.

The best performing catalyst, organosilylated sulphur containing K10, was also successfully regenerated by washing with toluene, giving in a subsequent test at 90 % conversion level slightly lower selectivity, 88 % in comparison to 95 % for the fresh catalyst.

Acknowledgements

AFP and CF acknowledge Fundação para a Ciência e a Tecnologia (FCT) (ref. PTDC/BII-BIO/30884/2017, UID/QUI/50006/2019 and DL57/2016 - Norma transitória), for financial support. The research visit of Nikolai Li-Zhulanov to Åbo Akademi University was supported by the EDUFI Fellowship programme, funded by the Finnish National Agency for Education.

R**eferences**

[1] I. V. Ilina, K.P. Volcho, V. V. Zarubaev, N. F. Salakhutdinov, RU2664 728 (2017).

[2] M. Stekrova, P. Mäki-Arvela, N. Kumar, E. Behvaresh, A. Aho, Q. Balme, K. P. Volcho, N. F. Salakhutdinov, D. Yu. Murzin, J. Mol. Catal. A: Chem. 410 (2015) 260-270.

[3] E. Kholkina, P. Mäki-Arvela, C. Lozachmeuer, R. Barakov, N. Shcherban, D. Yu. Murzin, Prins cyclisation of (-)-isopulegol with benzaldehyde over ZSM-5 based micro-mesoporous catalysts for production of pharmaceuticals, Chin. J. Catal. DOI:S1872-2067(19)63305-X.

[4] A. Yu. Sidorenko, A. V. Kravtsova, A. Aho, I. Heinmaa, K. P. Volcho, N. F. Salahutdinov, V. E. Agabekov, D. Yu. Murzin, ChemCatChem 10 (2018) 3950-3954.

[5] I. V. Ilyina, V. V. Zarubaev, I. N. Lavrentina, A. A. Shtro, I. L. Esaulkova, D. V. Korchagina, S. S. Borisevich, K. P. Volcho, N. F. Salakhutdinov, Bioorg. Medicin. Chem. Let. 28 (2018) 2061-2067.

[6] J. S. Yadav, B. V. Subba reddy, A. V. Ganesh, G. G. K. S. Narayana, Kumar, Tetrahedr. Lett. 51 (2010) 2963-2966.

[7] Y. Nagatani, K. Kawashima, Synthesis 147 (1978).

[8] P.Mäki-Arvela, N. Kumar, V. Nieminen, R. Sjöholm, T. Salmi, D. Yu. Murzin, J. Catal. 225 (2004) 155-169.

[9] E. Nazimova, A. Pavloa, O. Michalchenko, I. I'lina, D. Korchagina, T. Tolstikova, K. Volcho, N. Salakhutdinov, Med. Chem. Res. 25 (2016) 1369-1383.

[10] M. N. Timofeeva, V. N. Pancheno, K. P. Volcho, S. V. Zakusin, V. V. Krupskaya, A. Gil, O. S. Mikhalchenko, J. Mol Catal. A: Chem. 414 (2016) 160-166.

[11] I. V. Il'ina, D. V. Korshagina, K.P. Volcho, N. F. Salakhutdinov, Russ. J. Org. Chem. 46 (2010) 1002-1005.

[12] K. R. Reddy, K. Kishore, L. F. Silva Jr, J. Braz. Chem. Soc. 24, 9 (2013) 1414-1419.

[13] A. Yu. Sidorenko, A. V. Kravtsova, J. Wärnå, A. Aho, I. Heinmaa, I.V. Il'ima, K. P. Volcho, N. F. Salakhutdinov, D. Yu. Murzin, V. E. Agabekov, Mol. Catal. 453 (2018) 139-148.

[14] G. Baishya, B. Sarmah, N. Hazarika, N., Synlett.24 (2013) 1137-1141.

[15] A.Yu. Sidorenko, A.V. Kravtsova, A. Aho, I. Heinmaa, J. Warna, H. Pazniak, K.P.Volcho, N.F. Salakhutdinov, D.Yu. Murzin, V.E. Agabekov, J. Catal., 374 (2019) 360 – 377.

[16] J. Nowicki, K. Jaroszewska, E. Nowakowska-Bogdan, M. Szmatola, J. Olowska, Mol. Catal. 454 (2018) 94-103.

[17] S. M. Silva, A. F. Peixoto, C. Freire, Appl. Catal. A, Gen. 568 (2018) 221-230.

[18] M. M. Aboelhassan, A. F. Peixoto, C. Freire, New J. Chem. 41 (2017) 3595-3605**.**

[19] P. Pasbakhsh, R. de Silva, V. Vahedi, G. J. Churchman, Clay Miner. 51 (2016) 479-487.

[20] B. Duleba, E. Spišák, F. Greškovič, Procedia Eng. 96 (2014) 75 – 80.

[21] M. Tangestanifard, H. S. Ghaziaskar, Catalysts 7 (2017) 2-11.

[22] N.A. Negm, G.H. Sayed, F.Z. Yehia, O.I. Habib, E.A. Mohamed, J. Mol. Liq. 234 (2017) 157-163.

[23] S. M. Silva, A. F. Peixoto, C. Freire, Renew. Energy. DOI:10.1016/j.renene.2019.08.073.

[24] I.K. Mbaraka, D.R. Radu, V.S.-Y. Lin, B.H. Shanks, J. Catal. 219 (2003) 329-336.

[25] C. Emeis J. Catal. 141 (1993) 347-354.

[26] B. Delley, J. Chem. Phys. 92 (1990) 508-517.

[27] B. Delley, J. Chem. Phys. 113 (2000) 7756-7764.

[28] A. D. Becke, J. Chem. Phys. 98 (1993) 5648-5652.

[29] C. Lee, W. Yang, R. G. Parr Phys. Rev. B 37 (1988) 785-789.

[30] S. H. Vosko, L. Wilk, M. Nusair, Can. J. Phys. 58 (1980) 1200-1211.

[31] P. J. Stephens, F. J. Devlin, C. F. Chabalowski, M. J. Frischet, J. Phys. Chem. 98 (1994) 11623-11627.

[32] E. R. McNellis, J. Meyer, K. Reuter, Phys. Rev. B 80 (2009) 205414.

[33] B. Delley, Mol. Simul. 32 (2006) 117-123.

[34] B. Rafiei, F. A. Ghomi, J. Cryst. Min. 21 (2) (2013) 25-32.

[35] www.sigmaaldrich.com, date of access 15.6.2019.

[36] S. Prabakar, C. P. Whitby, A. M. Henning, G. Holmes, J. Am. Leather Chem. Ass. 111 (2016) 178-184.

[37] I. Muthuvel, B. Krishnakumar, M. Swaminathan, Ind. J. Chem. 51 (2012) 800-806.

[38] U. Unalan, G. Cerri, E. Marcuzzo, C. A. Cozzolino, S. Farris, RSC Adv. 4 (2014) 29393-29428.

[39] A. F. Peixoto, A. C. Fernandes, C. Pereira, J. Pires, C. Freire, Micropor. Mesopor. Mat. 219 (2016) 145-154.

[40] P. Bhagabati, C. T. Kumar, D. Khastgir, D. RSC Advances 5 (2015) 38209-38222.

[41] R. Ravisankar, S. Kiruba, P. Eswaran, G. Senthikumar, A.Chandrasekaran, E-journal of Chemistry 7 (1) (2010) S185-S190.

[42] S. Jana, S. Das, C. Ghosh, A. Maity, M. Pradham, Sci. Rep. 5 (2015) 1.

[43] M. Breugst, R. Grée, K.N. Houk, J. Org. Chem. 78 (2013) 9892–9897.

[44] K. Zheng, X. Liu, S. Qin, M. Xie, L. Lin, C. Hu, X. Feng, J. Am. Chem. Soc. 134 (2012) 17564-17573

[45] L. Sekerová, H. Černá, E. Vyskočilová, L. Červený, Reac Kinet Mech Cat 126 (2019) 869-878

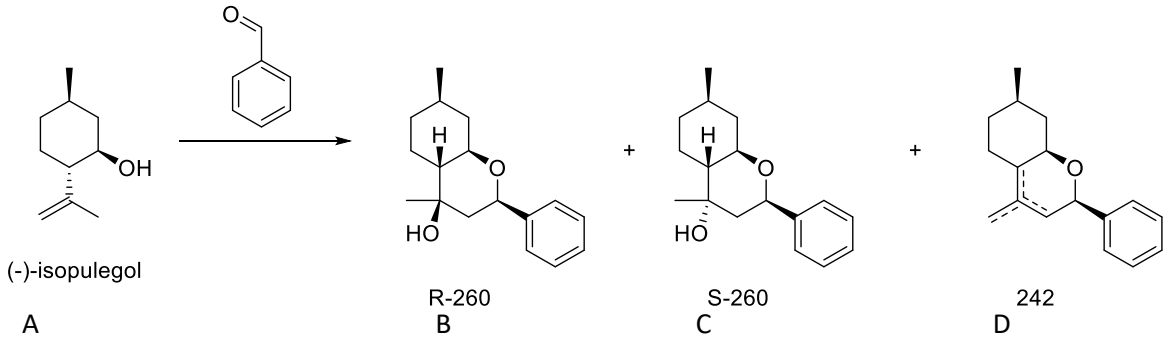

Scheme 1. Condensation of (-)-isopulegol (A) with benzaldehyde for production of chromenols (*4R*- and *4S*-diastereomers, denoted as B and C). The undesired dehydration product, D is also formed.

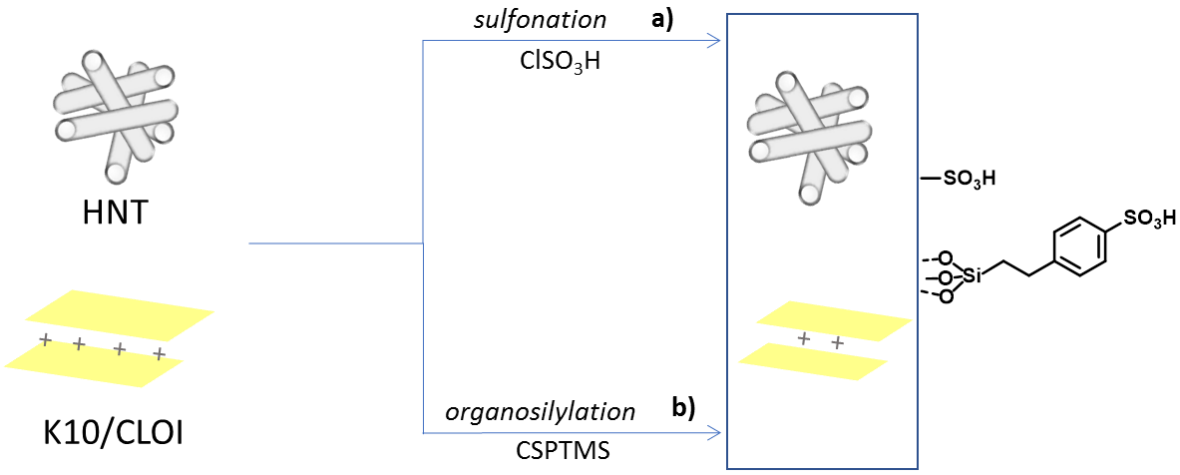

Scheme 2. Schematic representation of clays functionalization methods: a) organosilylation with CSP-TMS (2-(4-chlorosulphonylphenyl)ethyltrimethoxysilane), b) sulfonation with CSA (chlorosulfonic acid).

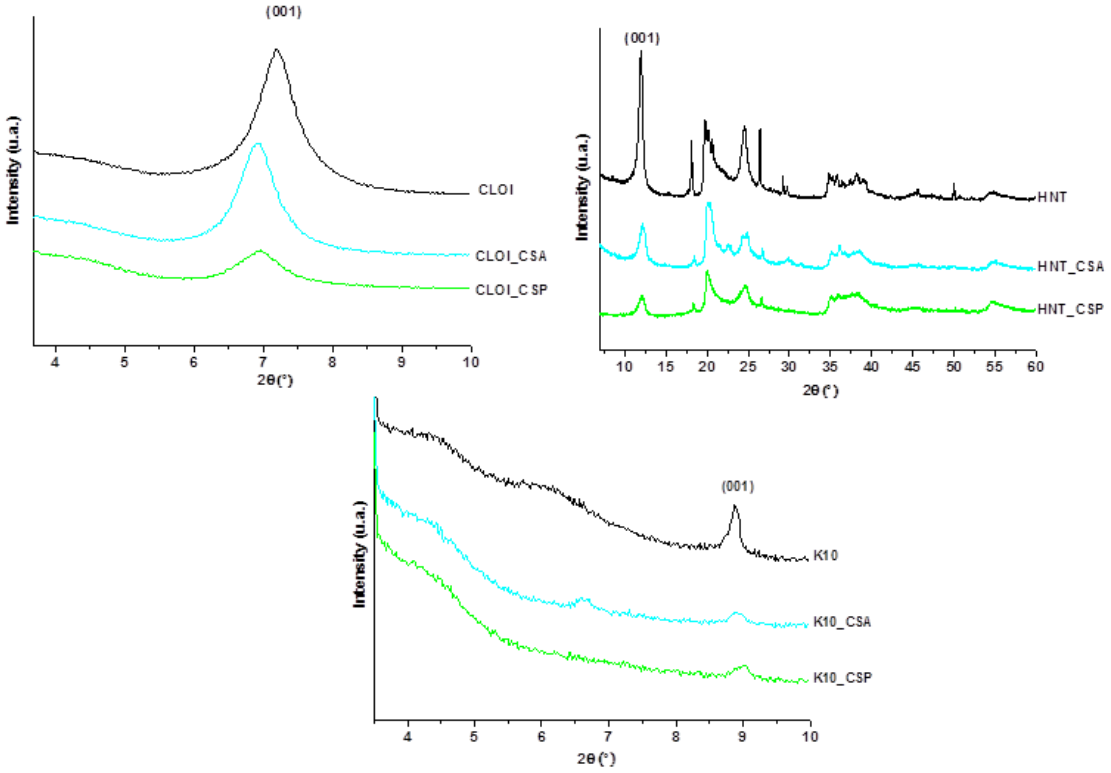

Fig. 1. X-ray powder diffraction patterns of the original and functionalized clays.

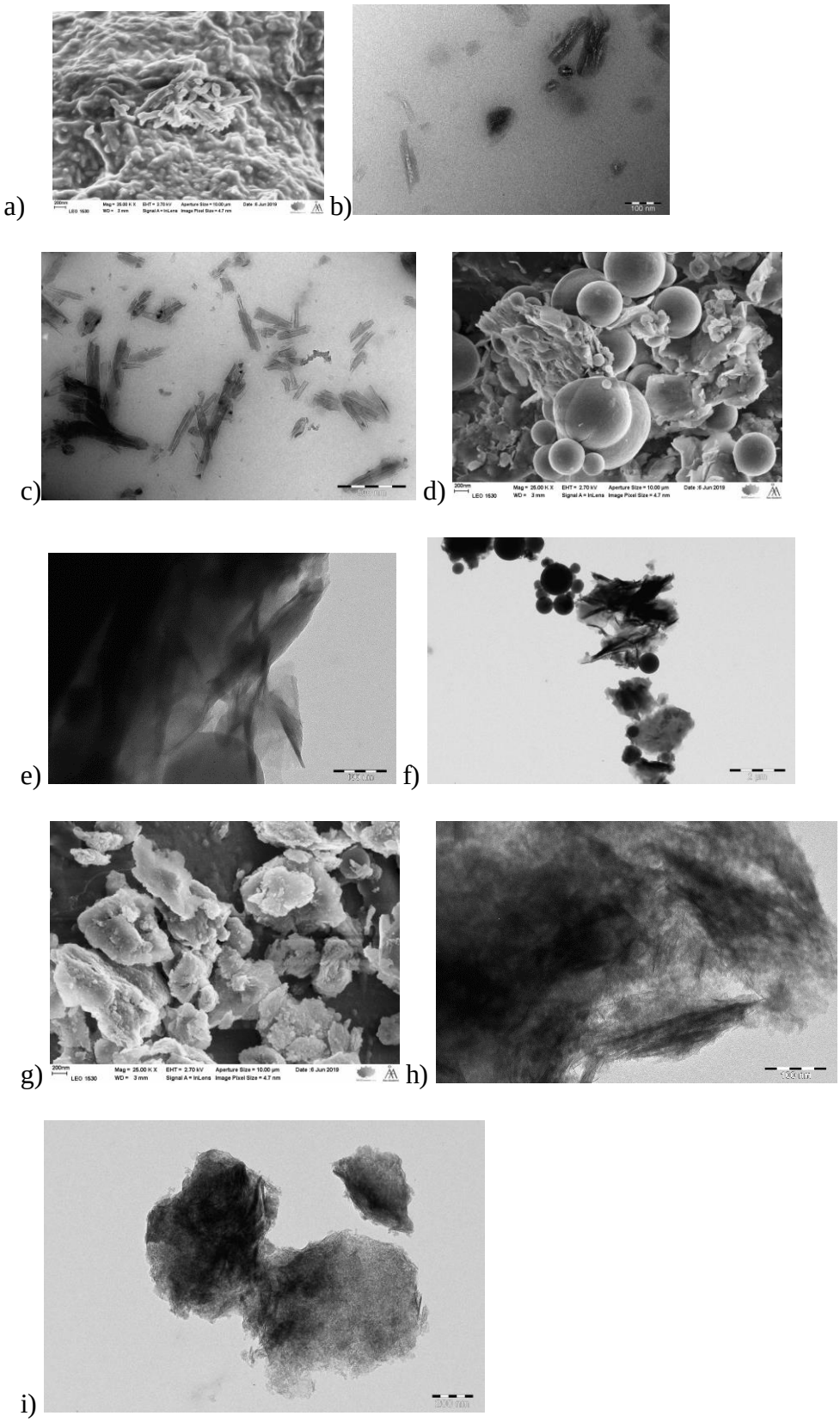

Fig. 2. a) SEM image of HNT_CSP, b) TEM images of HNT_CSP with scale 500 nm and c) with scale 100 nm, d) SEM image for CLOI_CSP, TEM images for CLOI_CSP e) scale 100 nm and f) 2000 nm CLOI_CSP and g) SEM of K10_CSP and TEM images for K10_CSP h) with scale 500 nm and i) scale 100 nm.

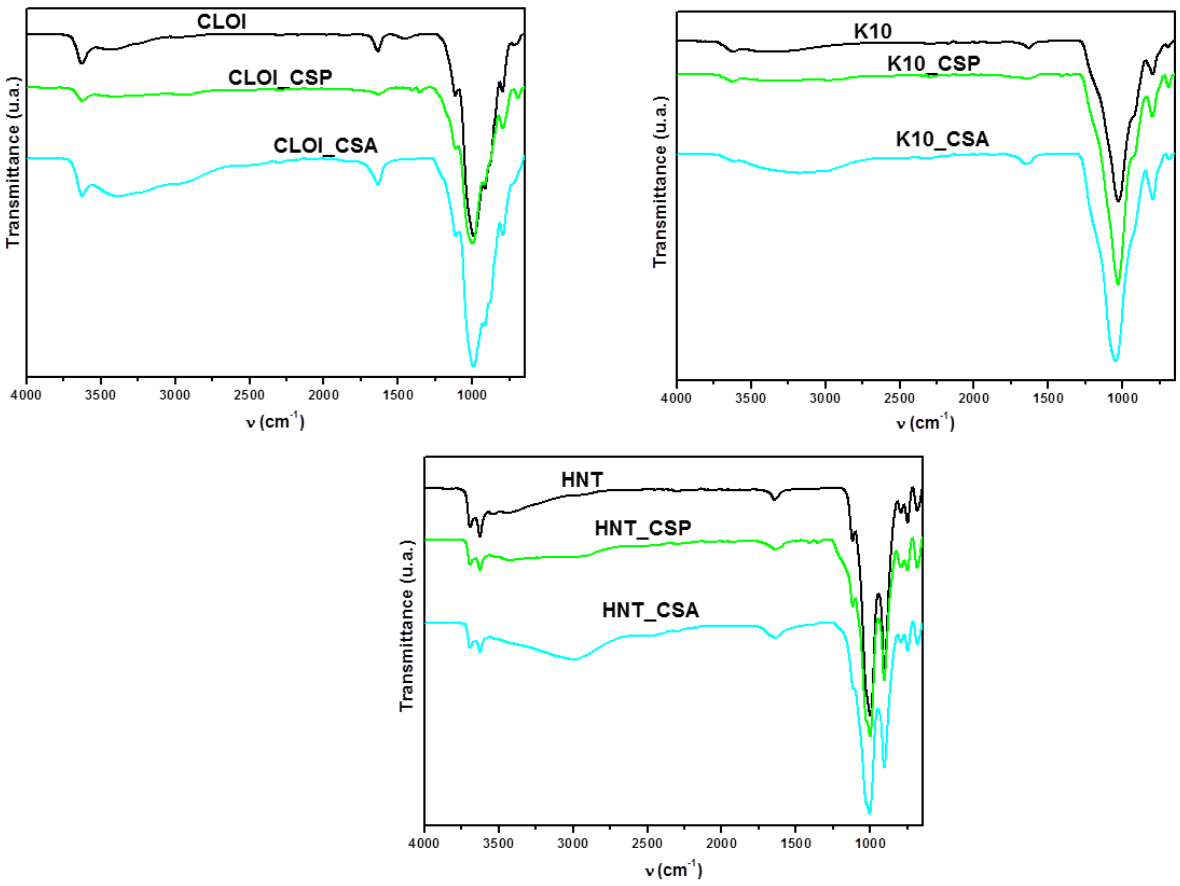

Fig. 3. FTIR-ATR full spectra of pristine and functionalized-CLOI, K10, HNT materials.

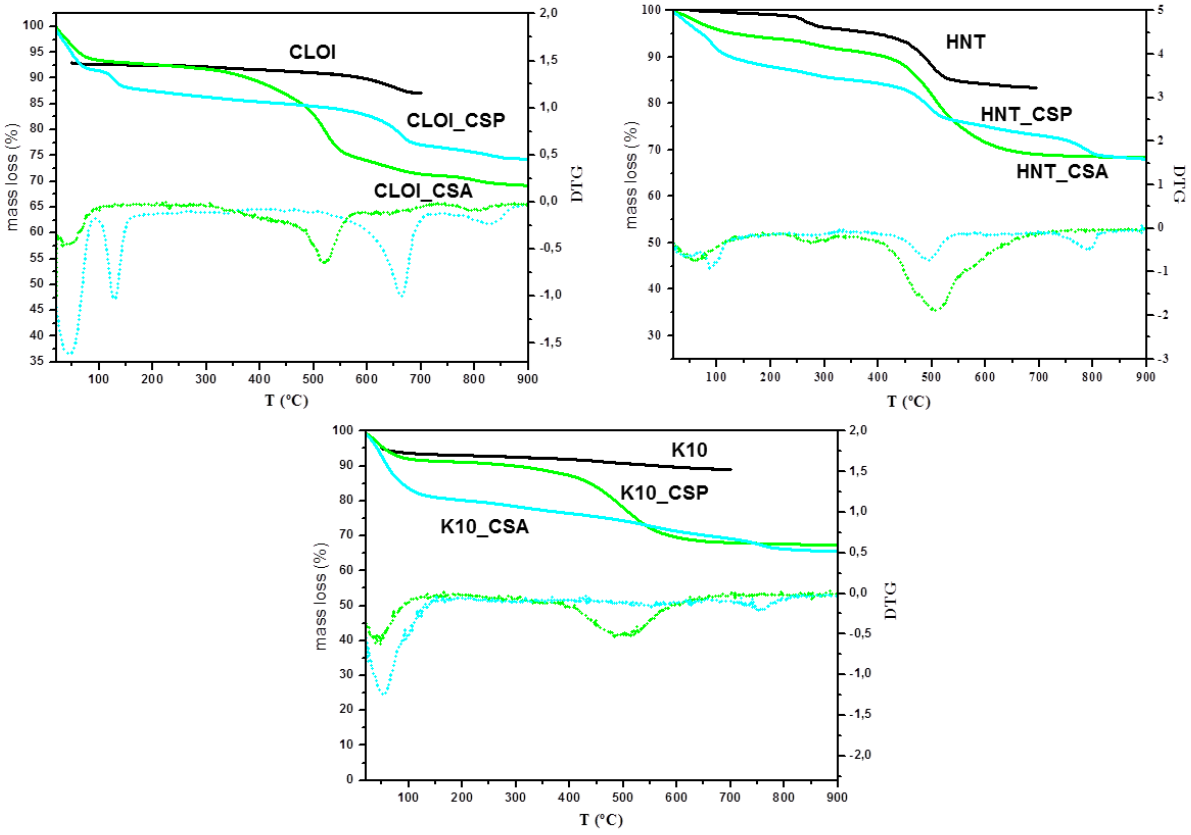

Fig. 4. Thermogravimetric curves (TG, bold lines) and the corresponding derivatives (DTG, dots) of pristine and functionalized clays.

a)

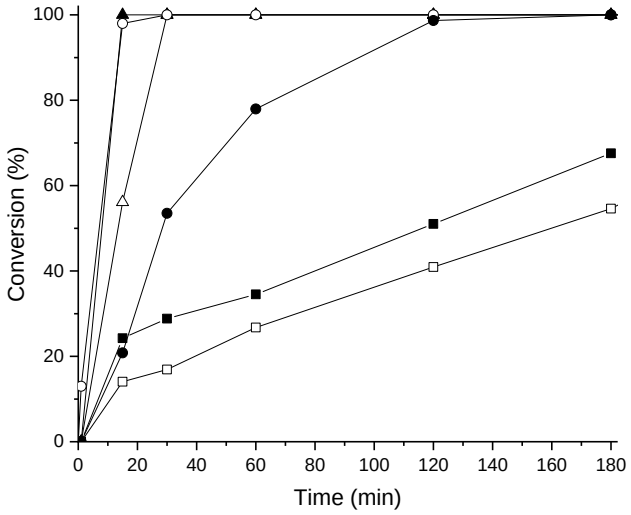

b)

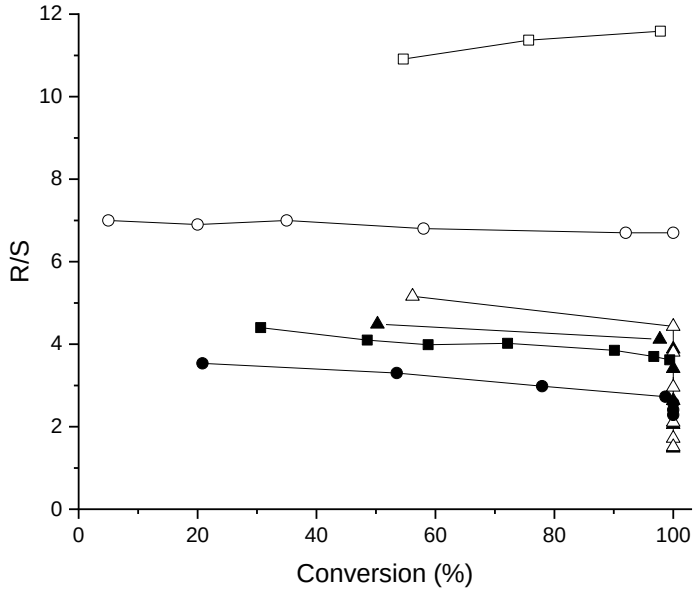

Fig. 5. Conversion as a function of time, *R/S* ratio as a function of conversion in condensation of (-)-isopulegol with benzaldehyde over HNT_CSA (■), HNT_CSP (□), K10_CSA (▲), K10_CSP (Δ), CLOI_CSA (●) and CLOI_CSP (o) catalysts at 70 ^{o}C in cyclohexane.

a)

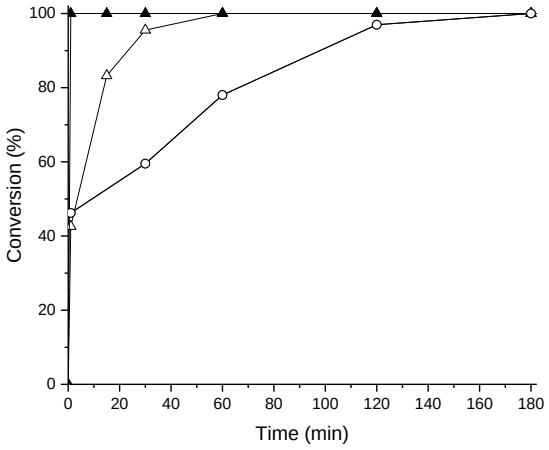

b)

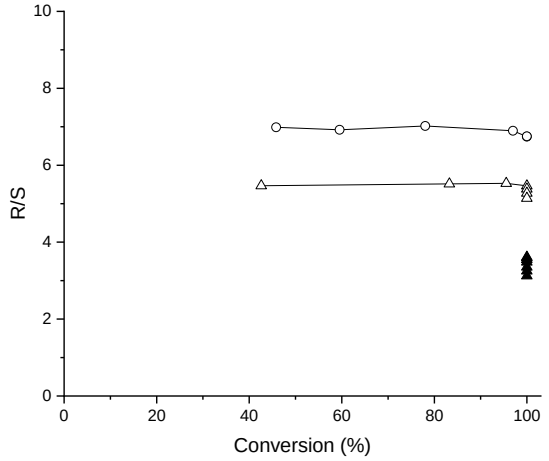

c)

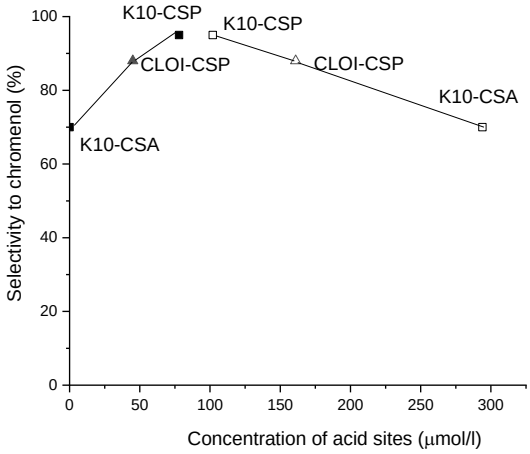

Fig. 6. a) Conversion of (-)-isopulegol as a function of time and b) *R/S* ratio as a function of conversion over K10_CSA (▲), K10_CSP (Δ) and CLOI_CSP (o), c) selectivity to chromenol at 90% conversion as a function of Brønsted and Lewis acid sites in different catalysts in Prins cyclisation of (-)-isopulegol with benzaldehyde at 30^{o}C. Notation: open symbol Brønsted acid and solid symbol Lewis acid.

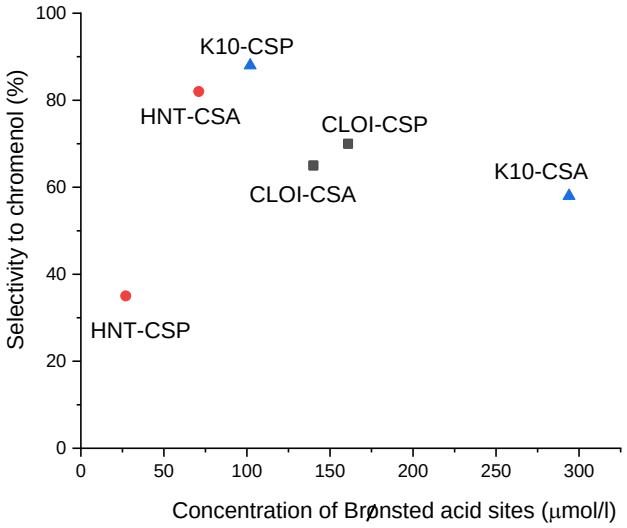

a)

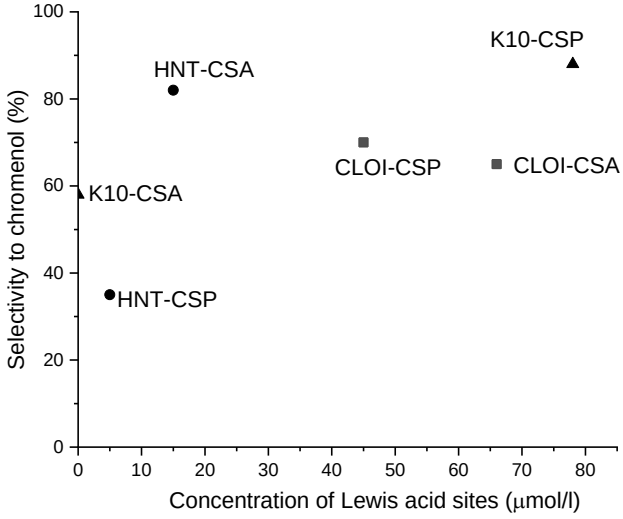

b)

Fig. 7. Selectivity to chromenol at 90% conversion as a function of Brønsted and Lewis acid sites in different catalysts in Prins cyclisation of (-)-isopulegol with benzaldehyde at 70°C.

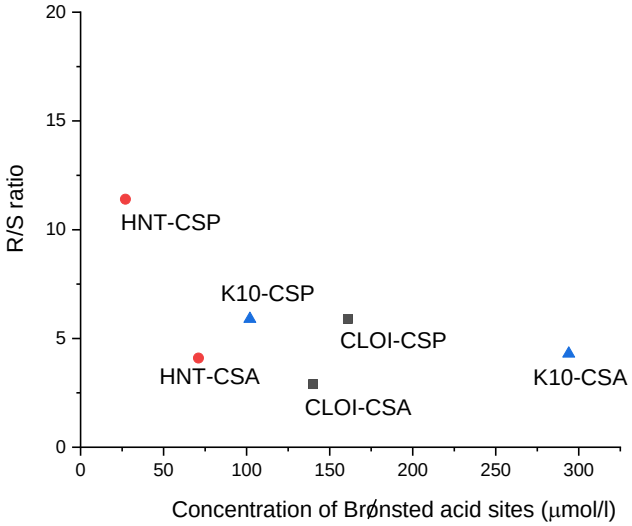

a)

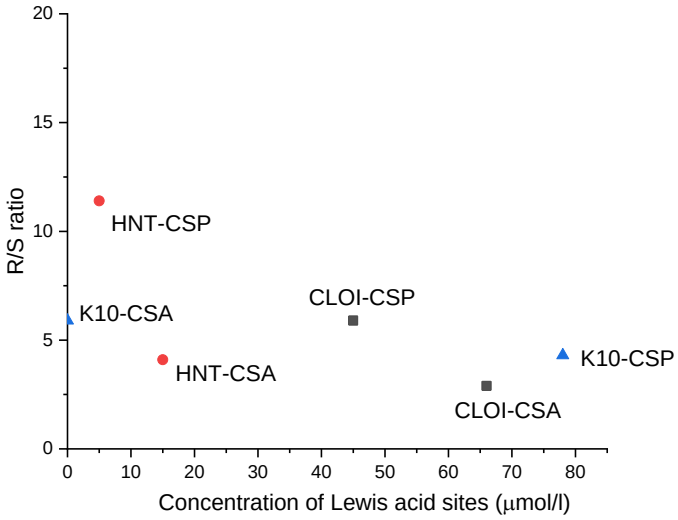

b)

Fig. 8. *R/S* ratio at 90 % conversion as a function of Brønsted and Lewis acid sites in different catalysts in Prins cyclisation of (-)-isopulegol with benzaldehyde at 70°C.

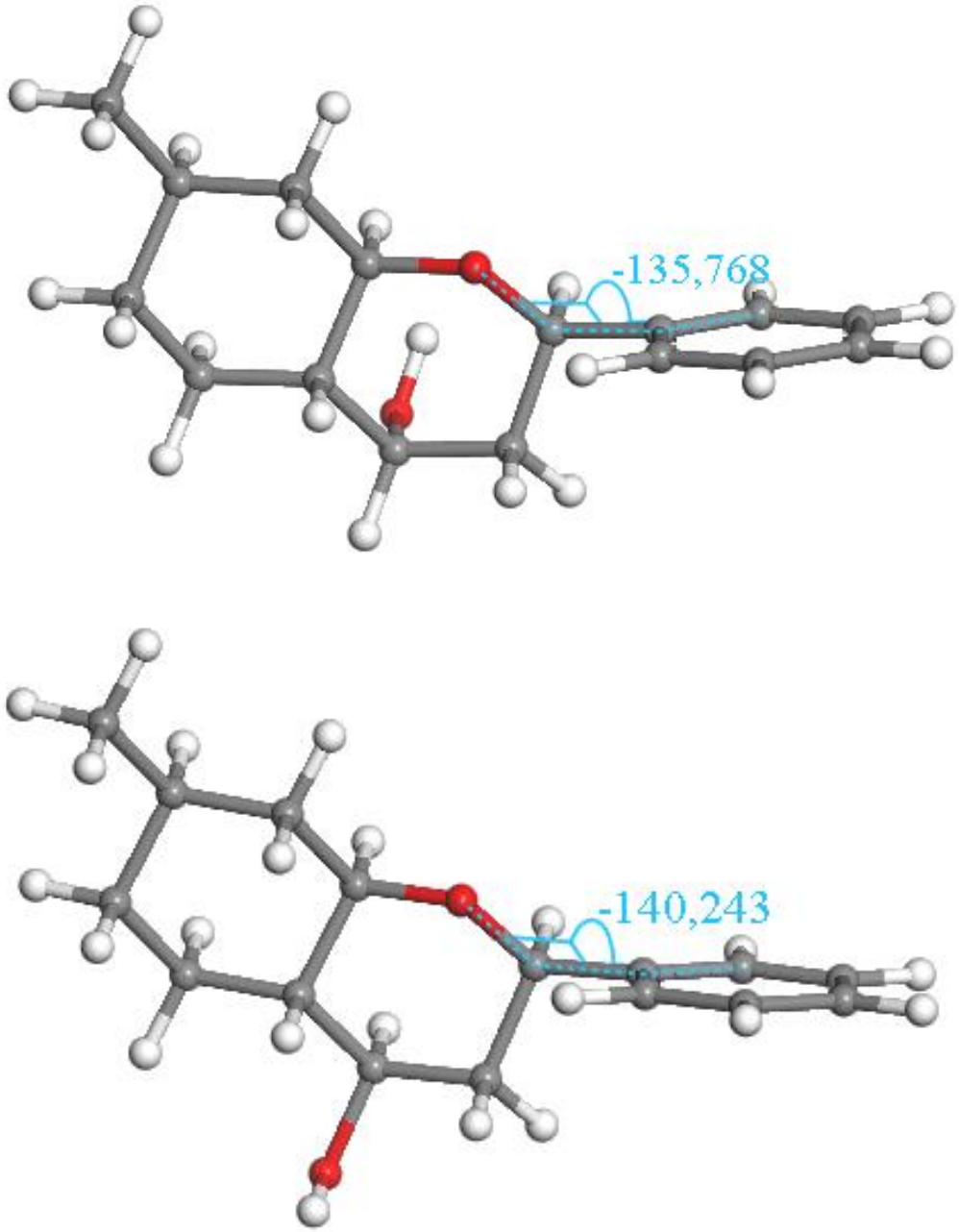

Fig. 9. Optimized structures of *R*-diastereomer of chromenol (below) and *S*-diastereomer (above).

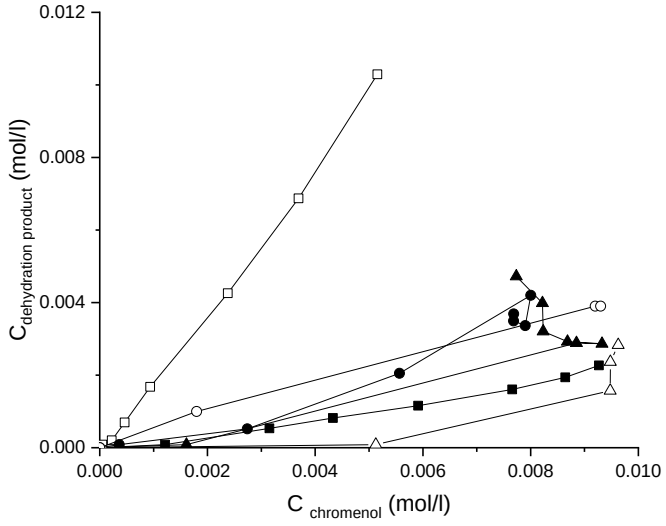

Fig. 10. Concentration of the dehydration products versus concentration of chromenol in condensation of (-)-isopulegol with benzaldehyde over HNT_CSA (■), HNT_CSP (□), K10_CSA (▲), K10_CSP (Δ), CLOI_CSA (●) and CLOI_CSP (o) catalysts at 70 ^{o}C in cyclohexane.

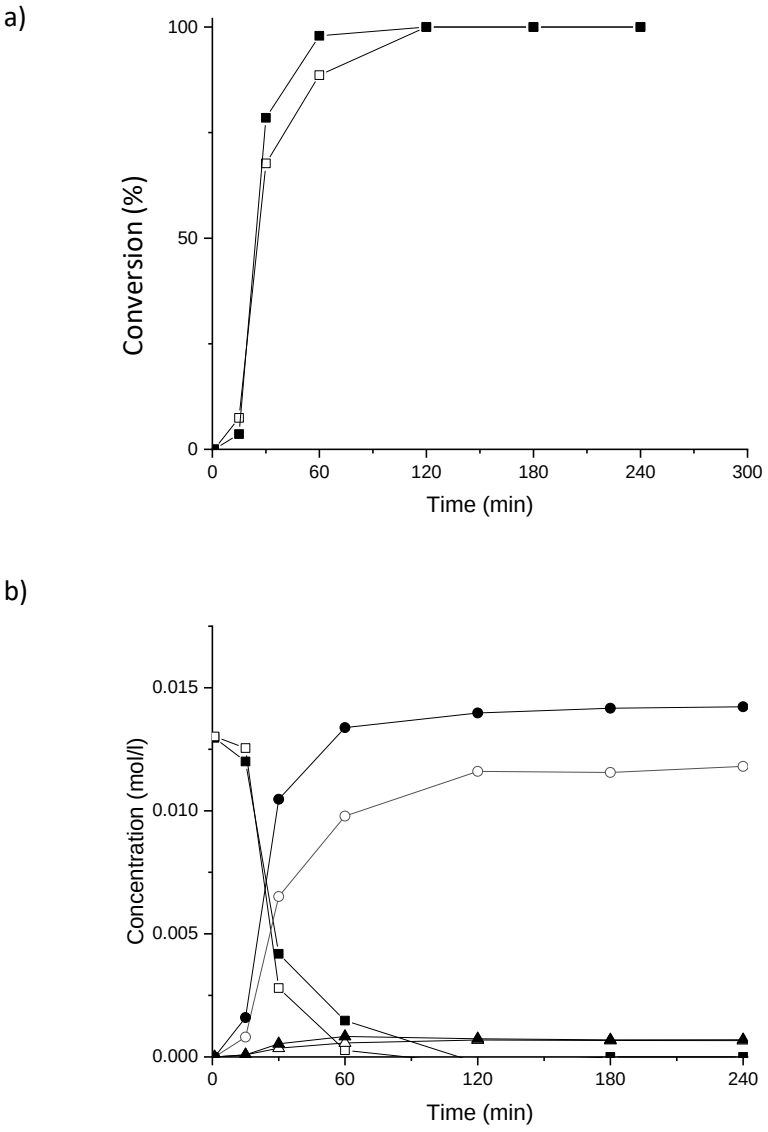

Fig. 11. Reproducibility test results from Prins cyclisation of (-)-isopulegol with benzaldehyde at 30º C with K10_CSP catalyst. Notation: a) conversion of (-)-isopulegol in experiment I (■) and II (□) and b) concentration profiles of (-)-isopulegol (), chromenol (o) and dehydration product (Δ) in experiment I (solid symbol) and II (open symbol).

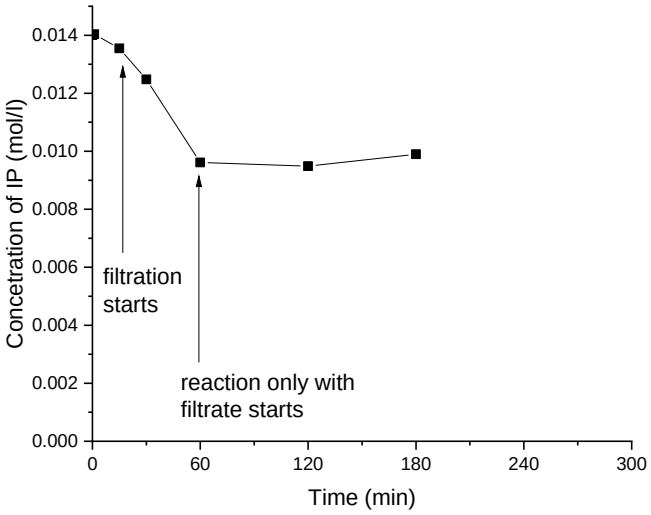

Fig. 12. Filtrate test with K10_CSP catalyst from Prins cyclisation of (-)-isopulegol with benzaldehyde at 30^{o} C. Filtration starts at 20 min, sample taken during filtration at 30 min, reaction starts with filtrate in the reactor at 60 min.

Table 1

XRD data of the pristine and functionalized clays.

Material	2theta (º)	*d* (Å)
HNT	12.0	7.4
HNT_CSA	12.1	7.3
HNT_CSP	12.1	7.3
K10	8.9	10.0
K10_CSA	8.9	9.9
K10_CSP	9.0	9.8
CLOI-Na^+	7.2	12
CLOI_CSA	6.9	13
CLOI_CSP	7.0	13

Table 2

Textural properties, chemical composition by elemental analysis and sulphur surface content by XPS.

Entry	**Material**	S_{BET} (m^2/g)	V_{pore}[a] (cm^3/g)	d_{pore}[b] (nm)	Elemental Analysis (mmol/g)		XPS(mmol/g)
					C	S	S
1	**HNT**	65[c]	-	-	0.04	-	-
2	HNT_CSA	7	0.057	3.6	0.15	0.84	1.15
3	HNT_CSP	10	0.075	12.0	6.48	0.83	1.25
4	**K10**	239[c]	-	-	0.07	-	-
5	K10_CSA	38	0.162	8.9	0.15	1.42	1.81
6	K10_CSP	155	0.245	3.7	9.73	1.21	0.50
7	**CLOI**	720[c]	-		0.15	-	-
8	CLOI_CSA	13	0.03	3.6	0.15	1.05	0.90
9	CLOI_CSP	5	0.049	3.6	10.06	1.31	0.59

[a] $V_{pore} = V_{total}$ ($p/p0 = 0.99$), $V_{micro} \sim 0$; [b] pore size; [c] Values from literature ref: [32]

Table 3
Surface atomic percentages of different elements determined by XPS for pristine and functionalized HNT, K10 and CLOI catalysts

Material	Surface atomic %									REF
	C 1s	**O** 1s	**Si** 2p	**Al** 2p	**Mg 1s**	**Fe 2p**	**Na1s**	**S 2p**	**Si/Al**	
HNT	5.9	63.7	15.5	14.9	-	-	-	-	1.04	[14]
HNT_CSP	27.7	49.9	11.2	8.8	-	-	-	2.4	1.27	
HNT_CSA	10.1	63.2	12.8	11.8	-	-	-	2.1	1.08	
K10	3.87	66.5	23.3	5.02	0.87	0.45		-	4.6	This
K10_CSP	10.8	61.7	21.5	4.04	0.75	0.31	-	0.92	5.3	work
K10_CSA	5.50	66.4	19.0	5.04	0.50	0.19	-	3.34	3.8	
Cloi-Na^+	8.64	59.1	19.8	8.06	1.95	-	2.45	-	2.5	This
Cloi_CSP	15.8	57.5	17.6	6.55	0.95	-	0.58	1.05	2.7	work
Cloi_CSA	3.90	66.4	18.8	7.58	1.14	-	0.55	1.68	2.5	

Table 4

Acidity of different catalysts determined by potentiometric titration and pyridine adsorption.

Material	Acidity (mmol H^+/g_{cat})[a]	Brønsted acid sites[b] ($\mu mol/g_{cat}$)	Lewis acid sites[b] ($\mu mol/g_{cat}$)
HNT	0.05	n.d.	n.d.
HNT_CSA	2.23	71	15
HNT_CSP	0.82	27	5
K10	0.22	n.d.	n.d.
K10_CSA	5.84	294	0
K10_CSP	0.80	102	78
CLOI	0.03	n.d.	n.d.
CLOI_CSA	1.78	140	66
CLOI_CSP	0.88	161	45

[a] by potentiometric titration. [b] pyridine adsorption by FTIR.

Table 5
Initial rate, conversion and selectivity to chromenol at 90% conversion (X= conversion), R/S ratio.

Clay	Initial reaction rate (mmol/min/g_{cat})	Temperature (^oC)	Time at 100% conversion (min)	Selectivity to chromenol at X= 90% (%)	R/S ratio at X= 90%
K10_CSA	Large	30	1	70	3.6
K10_CSA	Large	70	1	58	2.8
K10_CSP	0.28	30	60	95	5.5
K10-CSP	0.29	70	15	88	4.7
K10	0.002	30	60	87	5.5
HNT_CSA	0.11	70	240 (98% [a])	82	4.0
HNT_CSP	0.05	70	240 (99%[a])	35	11.5
CLOI_CSA	0.10	30	120	65	2.9
CLOI_CSP	0.21	70	180	88	6.8
CLOI_CSP	0.42	30	30	70	6.9

[a] in parenthesis conversion given at the specific time

Table 6
Quantum mechanically calculated thermodynamic quantities of R diastereomer of chromenol

T (K)	Entropy S (cal/mol*K)	Heat capacity Cp	Enthalpy H (kcal/mol)	Free energy G
275.00	106.151	46.679	178.404	149.212
298.15	110.090	50.860	179.533	146.709
300.00	110.406	51.196	179.627	146.505
325.00	114.684	55.753	180.964	143.692
350.00	118.982	60.288	182.415	140.771
375.00	123.294	64.751	183.978	137.743

Table 7
Quantum mechanically calculated thermodynamic quantities of 7 diastereomer of chromenol

T (K)	Entropy S (cal/mol*K)	Heat capacity Cp	Enthalpy H (kcal/mol)	Free energy G
275.00	103.117	45.870	179.042	150.685
298.15	106.991	50.058	180.153	148.253
300.00	107.301	50.396	180.246	148.055
325.00	111.516	54.965	181.563	145.320
350.00	115.756	59.516	182.994	142.479
375.00	120.015	63.998	184.538	139.532